The Journal of Clinical Pharmacology
2022, 62(3) 385–396

DOI: 10.1002/jcph.1972

Prediction of Moxifloxacin Concentrations in Tuberculosis Patient Populations by Physiologically Based Pharmacokinetic Modeling

Carlijn H. C. Litjens, PhD[1,2], Laurens F. M. Verscheijden, MSc[2], Celine Bolwerk, MSc[1], Rick Greupink, PharmD, PhD[2], Jan B. Koenderink, PhD[2], Petra H. H. van den Broek[2], Jeroen J. M. W. van den Heuvel[2], Elin M. Svensson, PhD[1,3], Martin J. Boeree, MD, PhD[4], Cecile Magis-Escurra, MD, PhD[4], Wouter Hoefsloot, MD, PhD[4], Reinout van Crevel, MD, PhD[5], Arjan van Laarhoven, MD, PhD[5], Jakko van Ingen, MD, PhD[6], Saskia Kuipers, MD, PhD[6], Rovina Ruslami, MD, PhD[7,8], David M. Burger, PharmD, PhD[1], Frans G. M. Russel, PharmD, PhD[2], Rob E. Aarnoutse, PharmD, PhD[1], and Lindsey H. M. te Brake, PhD[1]

Abstract

Moxifloxacin has an important role in the treatment of tuberculosis (TB). Unfortunately, coadministration with the cornerstone TB drug rifampicin results in suboptimal plasma exposure. We aimed to gain insight into the moxifloxacin pharmacokinetics and the interaction with rifampicin. Moreover, we provided a mechanistic framework to understand moxifloxacin pharmacokinetics. We developed a physiologically based pharmacokinetic model in Simcyp version 19, with available and newly generated in vitro and in vivo data, to estimate pharmacokinetic parameters of moxifloxacin alone and when administered with rifampicin. By combining these strategies, we illustrate that the role of P-glycoprotein in moxifloxacin transport is limited and implicate MRP2 as transporter of moxifloxacin-glucuronide followed by rapid hydrolysis in the gut. Simulations of multiple dose area under the plasma concentration–time curve (AUC) of moxifloxacin (400 mg once daily) with and without rifampicin (600 mg once daily) were in accordance with clinically observed data (predicted/observed [P/O] ratio of 0.87 and 0.80, respectively). Importantly, increasing the moxifloxacin dose to 600 mg restored the plasma exposure both in actual patients with TB as well as in our simulations. Furthermore, we extrapolated the single dose model to pediatric populations (P/O AUC ratios, 1.04-1.52) and the multiple dose model to children with TB (P/O AUC ratio, 1.51). In conclusion, our combined approach resulted in new insights into moxifloxacin pharmacokinetics and accurate simulations of moxifloxacin exposure with and without rifampicin. Finally, various knowledge gaps were identified, which may be considered as avenues for further physiologically based pharmacokinetic refinement.

Keywords

drug-drug interactions, modeling, moxifloxacin, physiologically based pharmacokinetics, tuberculosis

[1]Department of Pharmacy, Radboud Institute for Health Sciences & Radboudumc Center for Infectious Diseases, Radboud University Medical Center, Nijmegen, The Netherlands
[2]Department of Pharmacology and Toxicology, Radboud Institute for Molecular Life Sciences, Radboud University Medical Center, Nijmegen, The Netherlands
[3]Department of Pharmaceutical Biosciences, Uppsala University, Uppsala, Sweden
[4]Department of Pulmonary Diseases, Radboud Institute for Health Sciences & Radboudumc Center for Infectious Diseases, Radboud University Medical Center, Nijmegen, The Netherlands
[5]Department of Internal Medicine, Radboud Institute for Health Sciences & Radboudumc Center for Infectious Diseases, Radboud University Medical Center, Nijmegen, The Netherlands
[6]Department of Medical Microbiology, Radboud Institute for Health Sciences & Radboudumc Center for Infectious Diseases, Radboud University Medical Center, Nijmegen, The Netherlands
[7]TB/HIV Research Centre, Faculty of Medicine, Universitas Padjadjaran, Bandung, Indonesia
[8]Department of Biomedical Sciences, Division of Pharmacology and Therapy, Faculty of Medicine, Universitas Padjadjaran, Bandung, Indonesia

Submitted for publication 27 February 2021; accepted 18 September 2021.

Corresponding Author:
Carlijn H. C. Litjens, PhD, Department of Pharmacy, Radboud University Medical Center, Geert Grooteplein Zuid 10, 6525 GA Nijmegen, The Netherlands
Email: Carlijn.Litjens@radboudumc.nl

Tuberculosis (TB) is the leading cause of death from a single infectious agent. In 2018, an estimated 10 million people developed TB, and 1.45 million patients died.[1] Moxifloxacin is a bactericidal 8-methoxy-fluoroquinolone with efficacy against a wide range of infections, an acceptable safety profile, and significant exposures inside macrophages.[2,3] Moxifloxacin has different applications in TB treatment; first and foremost, it is 1 of the 2 most frequently recommended fluoroquinolones for patients with multidrug-resistant (MDR)-TB, and considered a critical component of MDR-TB treatment in general.[4] Second, it might improve the treatment outcomes of TB meningitis because of its bactericidal activity and relatively favorable cerebrospinal fluid (CSF) concentrations.[5,6] Third, it can be used in case of intolerance against first-line TB drugs.[7] Finally, it might have treatment-shortening potential in drug-susceptible TB if dosing could be optimized, especially when coadministered with rifampicin.[7]

Moxifloxacin is described to be primarily metabolized by the phase II enzymes uridine diphosphate-glucuronosyltransferases (UGT) 1A1 and sulfotransferase (SULT) 2A1, contributing for 14% and 35%, respectively.[8,9] A much lower metabolizing activity by UGT1A3, 1A7 and 1A9 has also been detected in vitro, but the contribution of these enzymes is clinically not relevant.[8] Of note, absorption, distribution and excretion of moxifloxacin has previously been suggested to be influenced by the activity of the efflux transporter P-glycoprotein (P-gp), for which moxifloxacin is a proposed substrate.[10,11] The aforementioned metabolic enzymes as well as P-gp are induced by rifampicin, the cornerstone drug in drug-sensitive TB.[12–17] Multiple daily doses of 400 mg of oral moxifloxacin result in total exposures (ie, area under the concentration-time curve [AUC] over the 24-hour dosing interval [$AUC_{0\text{-}24}$]) of ≈40 mg • h/L.[18–20] In controlled clinical studies, when coadministered with rifampicin, moxifloxacin plasma concentrations decrease by ≈30%.[19,20] Given the concentration-dependent activity of moxifloxacin, this decreased exposure might result in decreased activity and acquired resistance.[21]

Physiologically based pharmacokinetic (PBPK) modeling is a mechanistic approach in which system-specific parameters (eg, human anatomic and physiologic information) and drug-specific parameters (eg, physicochemical and [in vitro] pharmacokinetic information) are combined to predict absorption, distribution, metabolism and elimination (ADME) and the resulting pharmacokinetic (PK) profile of a compound. In this way, the influence of multiple covariates, including interacting drugs, dosing regimens and routes of administration, can be evaluated systematically in a mechanistic manner.[22] Furthermore, PBPK modeling can be used to extrapolate findings to various populations, including populations in which it is hard to obtain samples, such as pregnant women or children.

In this study, we combined in vitro, in silico, and clinical approaches and developed and validated a semimechanistic PBPK model. This was used to simulate moxifloxacin pharmacokinetics in vivo, including the drug-drug interaction with rifampicin for which we wanted to evaluate moxifloxacin dose adjustments. Furthermore, the model was used to predict the pharmacokinetics of moxifloxacin in pediatric populations and to gain more insight in the pharmacokinetics of moxifloxacin in general. Finally, we aimed to identify knowledge gaps hindering further improvements to PBPK modeling.

Methods

In Vitro ADME Parameters of Moxifloxacin

A detailed description of the in-house in vitro experiments to determine moxifloxacin in vitro ADME parameters—passive permeability, passive diffusion, P-gp transporter kinetics, glucuronidation by UGT1A1, and transport of moxifloxacin-glucuronide by multidrug resistance-associated protein (MRP) 2, can be found in Supplemental Information S1.

PBPK Modeling Platform

A PBPK model of moxifloxacin was developed using Simcyp simulator software version 19 release 1 (Certara UK Limited, Simcyp Division, Sheffield, United Kingdom). The model was built using data from in-house in vitro experiments combined with in vitro and clinical parameters from literature. A full PBPK distribution model with an Advanced Dissolution Absorption and Metabolism absorption module and permeability-limited liver model was used. Simulations were performed using Simcyp's virtual population of healthy North European Caucasian volunteers. Volume of distribution (V_d) was set at 261 L for healthy volunteers[23] (3.28 L/kg with an average weight of 80 kg in Simcyp) and adjusted to fit the reported V_d in an Indonesian patient population with tuberculosis of ≈120 L[19] (1.6 L/kg with an average weight of 80 kg in Simcyp). Each simulation was performed in 100 individuals. The age range and proportion of women in the virtual population were matched with the data sets used for validation. A linear-up-log-down calculation method was used for calculation of all predicted $AUC_{0\text{-}24}$ values.

PBPK Workflow

A 4-step approach was used to build and validate the moxifloxacin PBPK model and the drug-drug interaction with rifampicin (Figure 1).

First, the model was developed with a combination of in-house collected in vitro data and data already

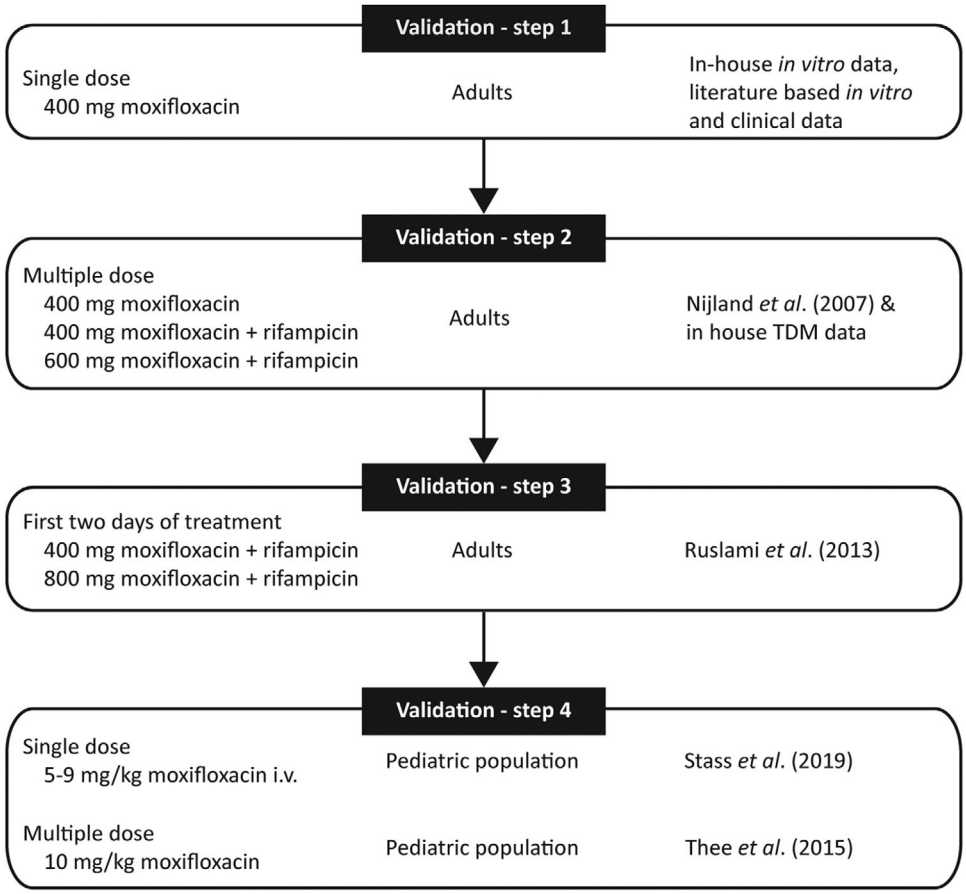

Figure 1. Work flow of the different validation steps of the moxifloxacin PBPK model in adult and pediatric populations. The type of the different data sources for the development and the human data to which the simulations were validated are described at the right of the figure. IV, intravenous; PBPK, physiologically based pharmacokinetic; TDM, therapeutic drug monitoring.

available from literature (in vitro and clinical). A single dose of 400 mg of moxifloxacin was simulated in healthy volunteers to determine the performance of the model.

Second, a multiple-dose regimen of moxifloxacin in a more TB-like population (V_d optimized) was simulated. We simulated the PK of multiple doses of 400 mg of moxifloxacin alone (5 doses once daily) and when administered with 600 mg rifampicin (10 doses and once-daily administration for both drugs). Finally, the simulated moxifloxacin dose was increased to 600 mg once daily to evaluate if this would compensate for the exposure reduction of ≈30% caused by rifampicin as seen in clinical studies.[19]

Third, rifampicin-moxifloxacin interaction simulations were performed during the first days of combined administration in TB treatment (2 doses of 400 or 800 mg of moxifloxacin with 600 mg of rifampicin once daily), which were compared with clinical data. We assumed that the concept and timing of increased rifampicin clearance over time, that is, the phenomenon of autoinduction with maximum autoinduction taking ≈14 and 24 days,[24,25] could be transferred to rifampicin-based induction of other phase I/II drug-metabolizing enzymes and transporters. This would entail that the moxifloxacin-rifampicin interaction in the first 2 days of treatment is influenced only by inhibition of enzymes and transporters caused by rifampicin. To simulate this, the moxifloxacin PBPK model (without induction) was combined with the rifampicin inhibition PBPK model.

The fourth and last step in the workflow involved PBPK model simulations in children using the virtual pediatric population incorporated in Simcyp. The ontogeny information as captured in the Simcyp pediatric module was used.[26] The ontogeny of UGT1A1 incorporated in Simcyp is mature at ≈3 months of postnatal age, which is in line with recent findings from Bhatt et al.[27] No ontogeny has yet been considered for SULT2A1 clearance in the version of Simcyp that was used; therefore, adult protein abundance is assumed, which is an arbitrary abundance, and incorporated by using the cytosolic enzyme cytochrome C1. This would be appropriate in the age range evaluated here, as SULT

abundance appears mature after the neonatal period.[28] Single intravenous doses of 9 (between 3 months and <2 years), 7 (≥2 to <6 years), and 5 mg/kg (and ≥6 to ≤14 years) of moxifloxacin in different healthy pediatric populations were simulated. Finally, multiple oral doses of 10 mg/kg in a pediatric population (7-14 years), with the V_d of moxifloxacin derived from the TB moxifloxacin model, was simulated.

Evaluation of Model Performance With Clinical Data

For all simulations, the performance of the model was checked by visual inspection of the mean PK curves, and by comparison of the simulated AUC and maximum plasma concentrations (C_{max}) with clinical data (an overview of literature provided clinical data can be found in Table S1), expressed by predicted/observed (P/O) ratios. According to general acceptance criteria, simulated mean AUC and C_{max} may not deviate more than 2-fold (0.5-2.0 × mean) from observed PK parameters.[29] For this purpose, AUC and C_{max} ratios were calculated by dividing the simulated geometric mean value by the observed value(s) (P/O ratios). As a more conservative approach, we also compared P/O ratios to the "20% decision rule"; differences in systemic drug exposure up to 20% (on a log-scale) are considered not clinically significant, resulting in a ratio range of 80% to 125%.

As a first validation of the model, single-dose simulations of 400 mg of moxifloxacin in healthy volunteers were compared with Stass and Kubitza[23] and Stass et al,[30] Sullivan et al,[31] and Lettieri et al[32] (Figure 1).

As a second validation, multiple dose simulation of moxifloxacin (400 mg) with and without rifampicin (600 mg) were compared to data from Nijland et al[19] and to routine collected therapeutic drug monitoring (TDM) data from patients with mycobacterial infections admitted to the Radboudumc-TB Expert Center (Dekkerswald, Groesbeek, The Netherlands) (Figure 1). As to the TDM data, data collection and analysis was performed retrospectively and in line with the General Data Protection Regulation of the European Union. Patients were included if they had been admitted between September 1, 2013, and January 31, 2019, received oral moxifloxacin (400 or 600 mg once daily) with or without coadministration of oral rifampicin (median dose, 1200 mg; range, 450-2000 mg, all once daily), and had at least 2 moxifloxacin concentration measurements at 1 day. Patients were categorized in 3 different groups: 400 mg of moxifloxacin once daily (group A), 400 mg of moxifloxacin once daily next to any dose of rifampicin (group B), and 600 mg of moxifloxacin once daily with any dose of rifampicin (group C); median rifampicin dose for both groups B and C was 1200 mg once daily (range, 450-2000 mg). Individual $AUC_{0\text{-}24}$ data were calculated with noncompartmental PK analyses or limited sampling formulas.[18] From these data, a geometric mean $AUC_{0\text{-}24}$ per subgroup was calculated. Individual plasma concentrations were plotted against time and a plasma concentration-time curve was fitted using locally estimated scatterplot smoothing regression in R Studio version 1.1.463 (RStudio, Inc, Boston, Massachusetts) after which a C_{max} was determined.

The third validation of the model was performed by simulation of 2 doses of 400 and 800 mg of moxifloxacin with 600 mg of oral rifampicin in the first days of treatment were compared to results by Ruslami et al,[5] in which patients were on combined treatment for a median of 2 (range, 1-3) days at the day of PK assessment (Figure 1).

As a last validation step, single-dose simulations of moxifloxacin (9, 7, and 5 mg/kg intravenously) without rifampicin in 3 healthy pediatric populations were compared to clinical data from children (between 3 months and <2 years, ≥2 to <6 years, and ≥6 to ≤14 years) with different kinds of infections published by Stass et al[33] (Figure 1). Also, simulation of multiple oral doses of 10 mg/kg of moxifloxacin in a pediatric population was compared to clinical data from (HIV-uninfected) children (between 7 and 15 years) with MDR-TB, described by Thee et al[34] (Figure 1).

Insight Into the Pharmacokinetics of Moxifloxacin: Routes of Elimination

In view of our aim to gain more insight in the pharmacokinetics of moxifloxacin, we combined available literature data, results from our in-house in vitro experiments, and analyses with our newly developed PBPK model, and compiled a conceptual overview of routes of elimination of moxifloxacin.

Results

In Vitro ADME Parameters of Moxifloxacin Based on In-House In Vitro Experiments

Moxifloxacin was tested as a substrate for the canalicular liver transporters transiently overexpressed in human embryonic kidney 293 cells, and it was confirmed to be a substrate for P-gp but not for breast cancer resistance protein, MRP2, and Bile Salt Export Pump (Figure S1). Previously, it has been shown that moxifloxacin is not a substrate for multidrug and toxin extrusion protein 1.[35] The mean passive permeability of moxifloxacin in Madin-Darby canine kidney cells was 11.5×10^{-6} (±0.92) cm/s as compared to 8.75×10^{-6} (± 1.5) cm/s for the reference compound propranolol. For the liver, the passive diffusion of moxifloxacin was 0.032 mL/min/10^{-6} hepatocytes. The initial intrinsic clearance of moxifloxacin by P-gp was 0.13 μL/min for intestine (Figure S2A) and 0.2 μL/min/million cells for liver. The initial intrinsic clearance of moxifloxacin

to moxifloxacin-acyl-glucuronide by UGT1A1 was 0.17 μL/min/mg microsomal protein (Figure S2B). Finally, moxifloxacin-glucuronide appeared to be a substrate for MRP2 (Figure S3).

Moxifloxacin Physicochemical and PBPK Parameters

An overview of parameter values used in the final model is presented in Table S2. All in-house obtained in vitro data were directly incorporated in the model, except for UGT1A1 activity, which had to be rescaled using Simcyp's reverse translation toolbox. Based on literature data, it was assumed that ≈8% of an oral moxifloxacin dose is not bioavailable[36] and ≈20% is renally excreted unchanged,[23] meaning that 70% of moxifloxacin is metabolized in the liver. Of the total clearance, 35% occurs via sulfation by SULT2A1,[23] leaving 35% of total clearance via glucuronidation by UGT1A1. As a result, both enzymatic processes were assumed to contribute equally to liver metabolism. By using the reverse translation toolbox, this resulted in an UGT1A1 intrinsic clearance of 0.058 μL/min/pmol enzyme. Finally, an additional clearance of 1 L/h had to be incorporated to reach the total reported clearance of 11.6 L/h.[23]

Volume of distribution at steady-state was calculated using the prediction method after Rodgers and Rowland,[37] which was optimized to match the reported distribution volume of 261 L (3.28 L/kg with an average weight of 80 kg in Simcyp) in healthy volunteers[23] and adjusted to fit the reported V_d in an Indonesian population of tuberculosis patients of ≈120 L (1.6 L/kg with an average weight of 80 kg in Simcyp).[19]

Rifampicin Physicochemical and PBPK Parameters

The rifampicin-MD "Inhibitor file" available in Simcyp was used. An overview of parameter values is presented in Table S3.

Induction of UGT1A1 by rifampicin was already incorporated in the Inhibitor file (maximal fold induction 3.2).[38] The half maximal inhibitory concentration (IC_{50}) of rifampicin for [^{3}H]-N-methyl quinidine transport by P-gp was 29 μM.[39] Since a low substrate concentration was used, the inhibitor constant of rifampicin for P-gp is considered to be equal to the IC_{50} based on the Cheng-Prusoff equation in case of competitive inhibition.[40] The IC_{50} (70 μM)[41] of rifampicin for estradiol glucuronidation by UGT1A1 was used since the substrate concentration was too high to equalize this to the inhibitor constant, and it was not clear whether there is competitive or noncompetitive inhibition. Data on time course and rifampicin concentration dependency for P-gp and SULT2A1 induction were not available. Therefore, the intestinal and liver relative expression factor of P-gp was increased by 3.5-fold to mimic the increase in expression at steady state after rifampicin treatment in vivo.[17,42] The same method was applied for SULT2A1, for which a 2.44-fold induction in mRNA expression after rifampicin treatment was described in human hepatocytes.[38]

Therapeutic Drug Monitoring Data

Moxifloxacin TDM data were available for 28 unique patients and were divided in 3 groups, oral moxifloxacin 400 mg only (group A, n = 4), oral moxifloxacin 400 mg with oral rifampicin (group B, n = 10) and oral moxifloxacin 600 mg with oral rifampicin (group C, n = 17). Patient characteristics per treatment group can be found in Table S4. The $AUC_{0\text{-}24}$ in group B decreased with 53% and the C_{max} with 19% upon coadministration with rifampicin compared to group A (Figure 2A-B), in line with findings from clinical studies.[19,20] After increasing the moxifloxacin dose to 600 mg, the $AUC_{0\text{-}24}$ in group C was only slightly lower (11%) compared to moxifloxacin alone, while the C_{max} was 42% higher compared to 400 mg of moxifloxacin alone (Figure 2C).

Single-Dose Simulation in Healthy Volunteers

Moxifloxacin single-dose simulation is presented in Figure 3. The simulated PK parameters and the shape of the curves were comparable with observed clinical PK parameters of moxifloxacin. [23,30–32] The predicted-to-observed ratio was 0.90 to 1.29 for $AUC_{0\text{-}\infty}$ and 0.53 to 1.20 for C_{max}.

Multiple-Dose Simulations in Adults With and Without Rifampicin

Multiple-dose simulations showed PK curve shapes in line with both literature and our TDM clinical data.[19] The simulated $AUC_{0\text{-}24}$ for the 400-mg dose without rifampicin was 35.8 mg • h/L (Figure 4A), and the $AUC_{0\text{-}24}$ and C_{max} ratio were between 0.74 to 0.86 and 0.64 to 0.97, respectively. In the simulation of 400 mg of moxifloxacin with daily rifampicin (600 mg oral) both the $AUC_{0\text{-}24}$ and C_{max} of moxifloxacin decreased by 41% and 23% to 21.3 mg • h/L and 2.3 mg/L, respectively (Figure 4B). The $AUC_{0\text{-}24}$ and C_{max} ratios were within the acceptance criteria (0.64-1.09 and 0.72-0.92, respectively). Of note, there was only a minor difference between simulating once-daily rifampicin (international guidelines) vs thrice weekly dosing of rifampicin as used in the study by Nijland et al[19] according to Indonesian guidelines (Figure S4). The simulation of 600 mg of moxifloxacin with 600 mg of rifampicin (Figure 4C), resulted in a comparable $AUC_{0\text{-}24}$ of 32.2 mg • h/L (ratio, 0.87) as well as a comparable C_{max} (ratio, 0.82) compared to our TDM data.

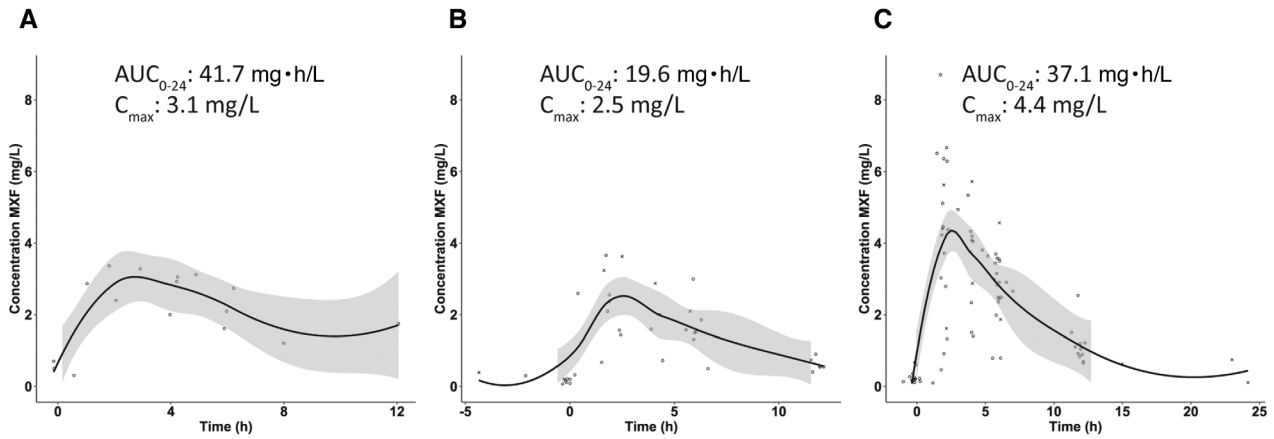

Figure 2. Pharmacokinetic curves of moxifloxacin with and without rifampicin coadministration of in-house collected therapeutic drug monitoring (TDM) data for 400 mg of moxifloxacin only (A), 400 mg moxifloxacin with any dose of rifampicin (B), and 600 mg of moxifloxacin with any dose of rifampicin (C); median rifampicin dose for both group B and C was 1200 mg once daily (range, 450-2000 mg). The x-axis indicates time after last dose. Open circles and crosses indicate measured individual data from in-house TDM data of patients with *Mycobacterium tuberculosis* or nontuberculous mycobacteria infections, respectively; the solid black lines indicate the fitted plasma concentration-time curve using locally estimated scatterplot smoothing regression; and the gray area represents the 95% confidence interval around the regression. $AUC_{0\text{-}24}$, area under the plasma concentration–time curve from time 0 to 24 hours; C_{max}, maximum plasma concentration.

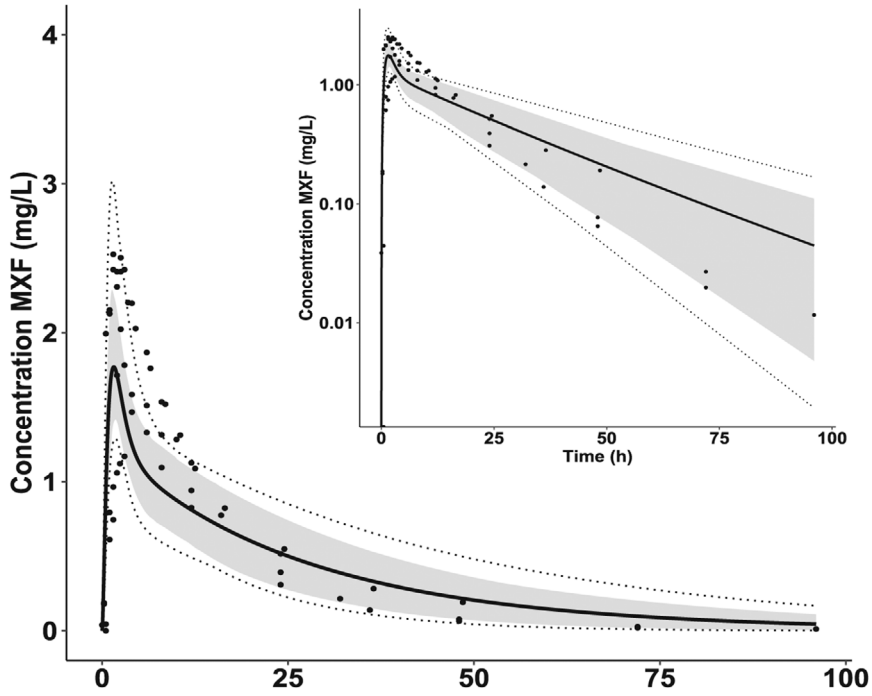

Figure 3. Simulation of moxifloxacin concentration-time profile after a 400-mg single oral dose in healthy volunteers. Solid black lines indicate simulation of the mean profile, the gray area represents the 90% confidence interval for interindividual variability, and the dotted lines indicate the minimum and maximum values after simulation. Dots indicate (geometric) mean observed data derived from clinical studies.[23,30–32] Log-transformed concentration-time data are depicted in the right upper corner (0 values were discarded). MXF, moxifloxacin.

Simulations in Adults With Rifampicin During the First Days of Treatment

To further validate the model, 2 doses of 400 and 800 mg of moxifloxacin coadministered with 600 mg of oral rifampicin were simulated, and results were compared to data in TB meningitis patients from Ruslami et al .[5] Figure 5A and 5B show that the mean simulation profile is in line with these data. The $AUC_{0\text{-}24}$ ratio between simulated and observed data was 1.23 and 1.14 for the 400- and 800-mg doses, respectively. The C_{max} ratio was 0.82 and 0.81 for the 400- and 800-mg doses, respectively.

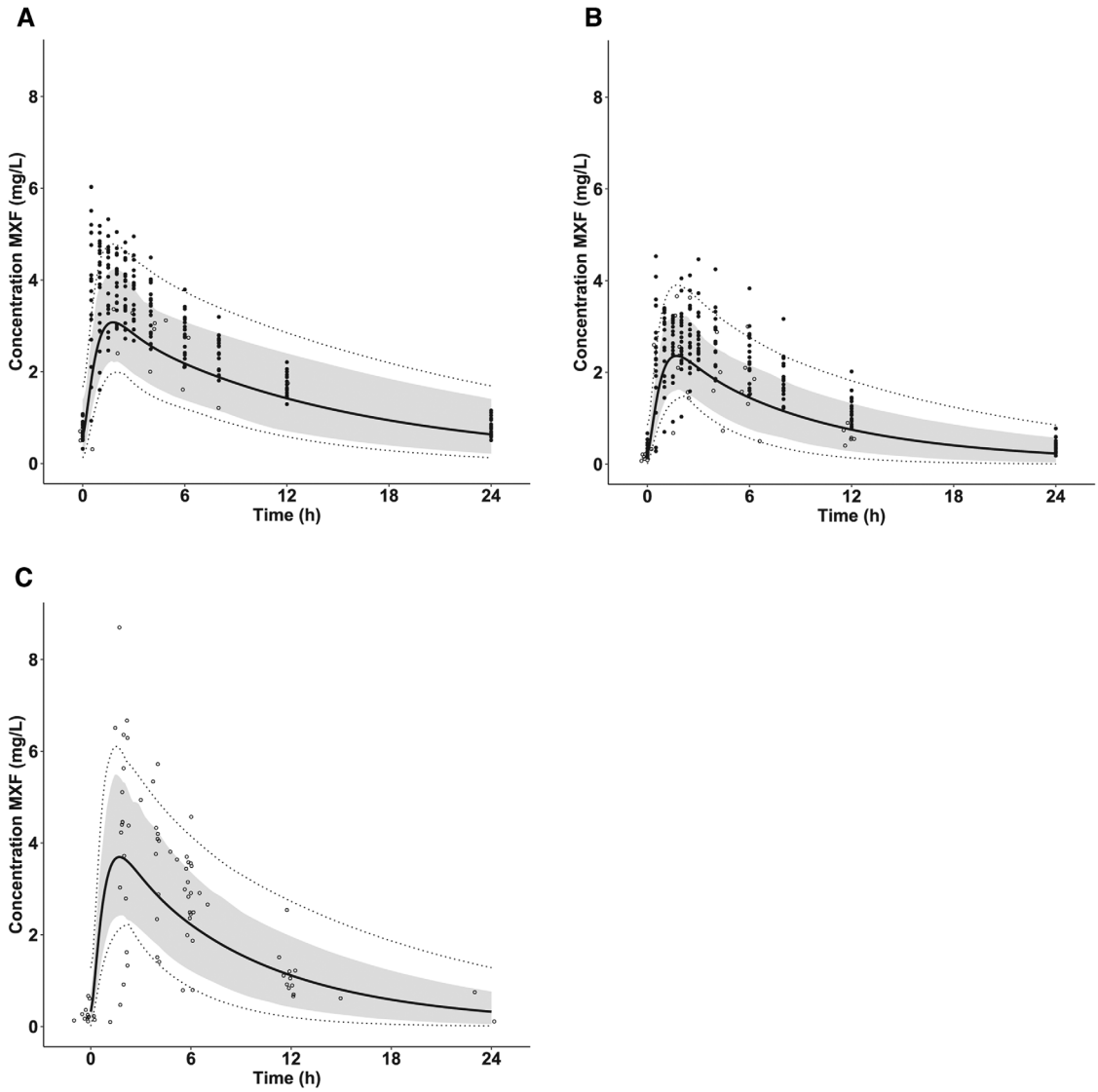

Figure 4. Simulations of moxifloxacin concentration-time profiles in patients with tuberculosis after multiple doses. The results relate to oral administration of 400 mg of moxifloxacin once daily for 5 days (A), 400 mg of moxifloxacin with 600 mg of rifampicin once daily for 10 days (B), and 600 mg moxifloxacin with 600 mg rifampicin once daily for 10 days (C). The x-axis indicates time after last dose. Solid black lines indicate simulation of the mean profile, the gray areas represent the 90% confidence interval for interindividual variability, and the dotted lines indicate the minimum and maximum simulation. Open circles and crosses indicate measured individual data from in-house therapeutic drug monitoring data of patients with *Mycobacterium tuberculosis* or nontuberculous mycobacteria infections, respectively, and closed circles indicate literature individual data.[19] MXF, moxifloxacin.

Simulations in Pediatric Populations

Figure 6A-C shows the simulation of a single intravenous dose of moxifloxacin in three healthy pediatric populations. All $AUC_{0\text{-}24}$ and C_{max} ratios were within the predefined acceptable ranges compared to the clinical data from Stass et al.[33] Figure 6D shows the simulations after multiple oral doses of moxifloxacin (10 mg/kg) in a pediatric population between 7 and 15 years. The simulated AUC from time 0 to 8 hours ($AUC_{0\text{-}8}$) and C_{max} values were in line with the reported value in a pediatric population with MDR-TB ($AUC_{0\text{-}8}$ ratio 1.51 and C_{max} ratio 1.56).[34] In addition, to understand the performance of mg/kg dosing in children, 10 mg/kg of moxifloxacin was modeled for 4 days in different age groups: infants, toddlers, preschool, middle childhood, young teens, and teens. The geometric mean moxifloxacin $AUC_{0\text{-}24}$ in children (≈50 mg • h/L irrespective of age group) is predicted to be higher compared to exposure in adults following a standard 400-mg daily dose, with moxifloxacin exposures in children, without rifampicin coadministration, remaining well above the pharmacologic threshold (ie, 40 mg • h/L) for all age groups (Figure S5).

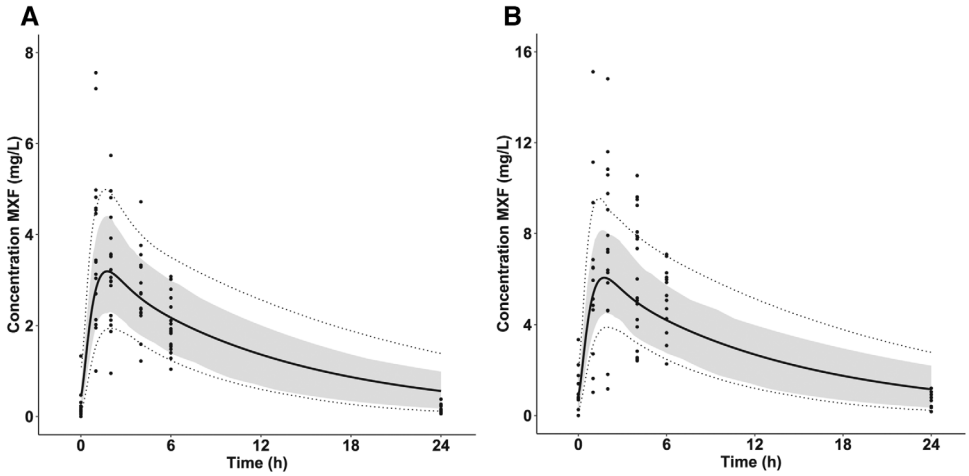

Figure 5. Simulations of moxifloxacin concentration-time profiles in patients with tuberculosis during the first 2 days of combined treatment. The results relate to oral administration of once-daily 400 mg of moxifloxacin with 600 mg of rifampicin (A), and 800 mg of moxifloxacin with 600 mg of rifampicin (B) during the first 2 days of treatment. The x-axis indicates time after the last dose. Solid black lines indicate simulation of the mean profile, the gray areas represent the 90% confidence interval for interindividual variability, and the dotted lines indicate the minimum and maximum simulation. Dots indicate measured individual data derived from literature.[5] MXF, moxifloxacin.

Figure 7 (and Table S5) show an overview of the comparison between moxifloxacin predicted and observed values of AUC ($AUC_{0-\infty}$, AUC_{0-24h} or AUC_{0-8h}) and C_{max} of all simulations performed.

Conceptual Overview of Moxifloxacin Routes of Elimination

Figure 8 gives a schematic overview of the moxifloxacin routes of elimination. A small part of the moxifloxacin dose is generally considered to be nonbioavailable[36]; for simplicity, this is shown as parent compound directly excreted in the feces.

Moxifloxacin and its sulfated (M1) and glucuronidated (M2) metabolites are partially excreted via the urine. The unbound fraction of moxifloxacin in plasma is ≈60% of moxifloxacin,[23] which would hypothetically result in a renal clearance of 3.6 to 4.2 L/h via glomerular filtration alone. As the renal clearance of moxifloxacin was reported to be 2.4 L/h, we assume that renal excretion occurs via glomerular filtration followed by partial tubular reabsorption. After oral administration of moxifloxacin, the renal clearances of M1 and M2 have been reported to be 13 and 9 L/h, respectively,[23] suggesting active excretion of these metabolites into the urine. Our study shows that moxifloxacin itself is a (moderate) substrate of P-gp, and its glucuronidated metabolite M2 a substrate of MRP2 mediating its biliary excretion. Finally, we hypothesize that the sulfated metabolite M1 is actively eliminated into bile by the breast cancer resistance protein, as this transporter preferentially exports sulfated conjugates rather than free compounds.[43,44]

Stass and Kubitza[23] described that ≈25% of a moxifloxacin dose is excreted as moxifloxacin, and 35% of a dose is found as M1 in feces, while M2 is not. In our in vitro study, we observed a low intrinsic clearance of moxifloxacin by P-gp (Figure S2), suggesting a low transporter affinity. Furthermore, sensitivity analyses of P-gp activity in our PBPK model showed hardly any influence on the elimination of moxifloxacin (AUC ratio with and without P-gp, 0.91). In accordance with Kaneko et al,[45] we suggest that biliary excretion of moxifloxacin through P-gp–mediated transport is only minor. In addition, we hypothesize that M2 is actively transported into the bile via MRP2, but will be hydrolyzed in the intestinal lumen back to moxifloxacin via gut bacterial proteases.[46] These considerations (Figure 8) lead to the following assumptions: (1) ≈35% of moxifloxacin is converted by UGT1A1 and excreted as M2, that is, 14% via the urine and 21% via the bile; and (2) M2 is subsequently hydrolyzed in the intestine and excreted as moxifloxacin in the feces.[23]

Discussion

Here, we present a semimechanistic PBPK model for moxifloxacin and its interaction with rifampicin. Furthermore, we demonstrate the effectiveness of moxifloxacin dose adjustments, with moxifloxacin dose increases from 400 to 600 mg once daily successfully restoring moxifloxacin plasma concentrations in our PBPK model as well as in clinical practice. Moreover, our PBPK model was able to adequately predict moxifloxacin exposures in healthy volunteers and in patients with TB with and without coadministration of rifampicin. Finally, we were able to predict moxifloxacin exposures in various pediatric patient populations following both single-dose and multiple-dose conditions.

The last goal of this study was to gain more insight in the pharmacokinetics of moxifloxacin. In our in vitro

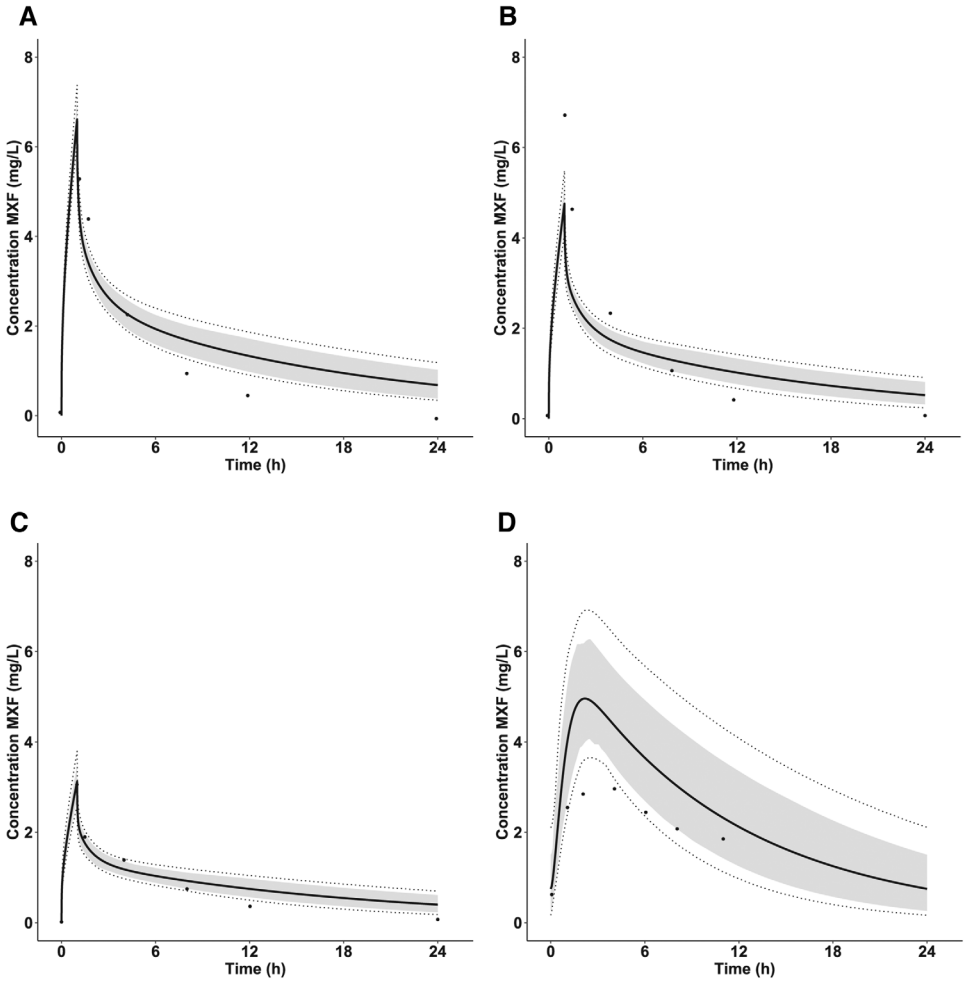

Figure 6. Simulations of moxifloxacin concentration-time profiles in children. Single-dose 9 mg/kg intravenous (IV) in children between 3 months and <2 years (A), single dose 7 mg/kg IV in children between ≥2 and <6 years (B), single dose 5 mg/kg IV in children between ≥6 and ≤14 years (C), and multiple doses of 10 mg/kg once daily oral in children with multidrug-resistant tuberculosis between 7 and 15 years for 5 days (D). The x-axis indicates time after last dose. Solid black lines indicate simulation of the mean profile, the gray area represents the 90% confidence interval for interindividual variability, and the dotted lines indicate the minimum and maximum simulation. Dots indicate measured data (geometric mean [A-C] and mean [D]) derived from literature.[33,34] MXF, moxifloxacin.

study we identified moxifloxacin as a substrate for P-gp, but our work also suggests that the contribution of P-gp to the excretion of moxifloxacin in vivo is only limited. We did not identify moxifloxacin as a substrate for MRP2 (Figure S1) nor for organic anion-transporting polypeptide (OATP) 1B1, OATP1B3, or OATP2B1 (data not shown), in our in vitro study, which is in contrast with previous findings in the literature.[10,47] However, we did find that MRP2 transports the moxifloxacin-glucuronide (M2). Based on this, we hypothesized, in agreement with Kaneko et al,[45] that not moxifloxacin itself, but moxifloxacin-glucuronide is transported from the liver to the intestines. This is followed by rapid hydrolysis by gut bacteria, resulting in the excretion of moxifloxacin in the feces,[45,46] similar to bilirubin deconjugation.[48] This theory is supported by the observation that moxifloxacin-glucuronide is excreted in the bile of rat liver perfusions.[47] Finally, in simulations during the first 2 days of treatment, rifampicin was not found to significantly impact moxifloxacin pharmacokinetics (data not shown), meaning that the interaction (ie, mediated only via UGT1A1 and P-gp inhibition at this point) is limited during the early days of combined treatment.

Our approach has some limitations, which may be considered as avenues for further PBPK refinement beyond the scope of our research. First, we had to make assumptions during model development and simulation, and introduced scaling factors in our PBPK model. For example, volume of distribution (based on the Rodgers et al[37] prediction method) and glucuronidation by UGT1A1 had to be rescaled based on clinical data. Furthermore, an additional clearance of 1 L/h had to be incorporated to match clinical observed

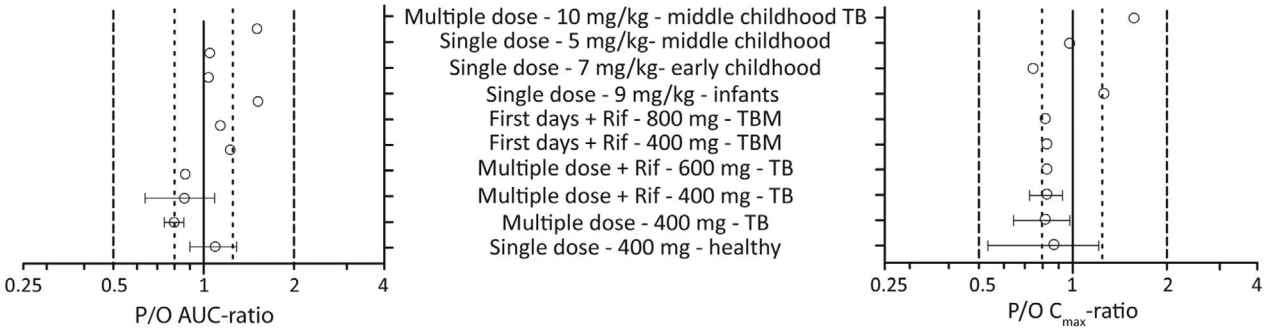

Figure 7. Overview of ratios between the predicted and observed area under the concentration-time curve (left) and the maximum concentration (right). Results are presented as mean ratios with range in case of multiple observed values.[5,19,23,30–34] The solid line at the x-axis represents no difference between the predicted and observed PK parameters AUC or C_{max} (ratio 1.0), the dotted lines represent the bioequivalence range between 0.8 and 1.25 and the dashed lines the range between 0.5 and 2. The *y*-axis represents the various dosing regimens in the different (age) groups. AUC, area under the plasma concentration–time curve; $AUC_{0-\infty}$, area under the plasma concentration–time curve from time 0 to 24 hours; or AUC_{0-8}, area under the plasma concentration–time curve from time 0 to 8 hours; C_{max}, maximum concentration, Rif, rifampicin, TB, tuberculosis, TBM, tuberculous meningitis.

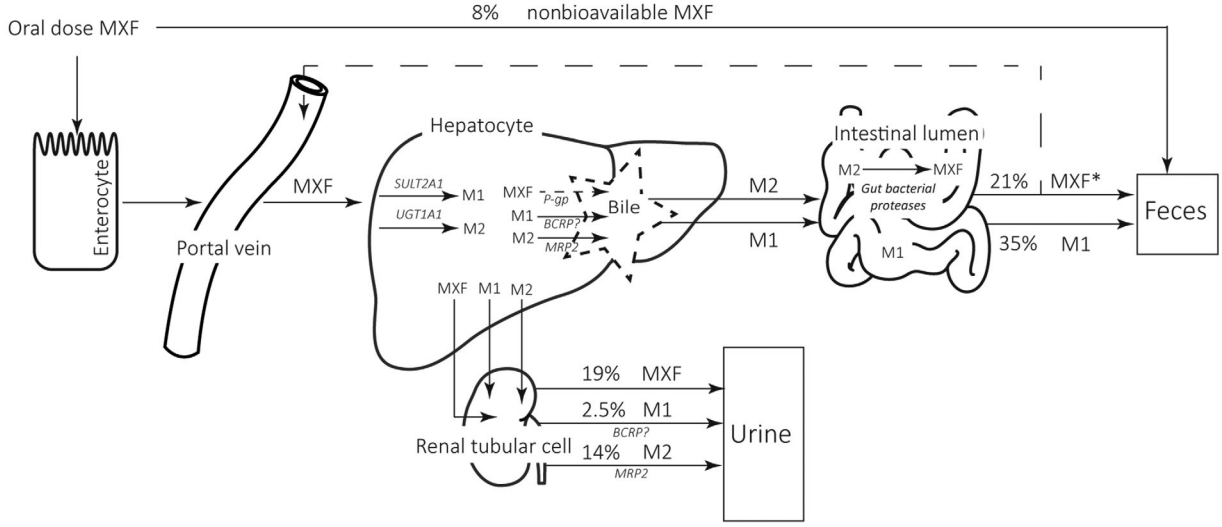

Figure 8. Conceptual overview of moxifloxacin routes of elimination. *Calculated based on considerations and assumptions on the role of UGT1A1. MXF, moxifloxacin; M1, sulfated metabolite; M2, glucuronidated metabolite; UGT1A1, uridine diphosphate-glucuronosyltransferase 1A1.

clearance. Yet our model is "fit for purpose"; it correctly predicts moxifloxacin pharmacokinetics in different populations. Second, as another limitation, data on turnover rates of P-gp and SULT2A1 are lacking and had to be incorporated in the rifampicin interaction model in a semimechanistic manner (ie, by increasing the relative expression factor value). Therefore, in our multiple-dose PBPK model, it is assumed that the interaction between rifampicin and moxifloxacin is always at maximum and independent of development over time and rifampicin exposure. We assume no problems in extrapolating our multiple-dose model to higher rifampicin dosing regimens, which are considered to be important in increasing efficacy in TB treatment, since available data suggest that a 300-mg rifampicin dose already results in maximum induction.[49] Because of a lack of available data, we also could not incorporate a theoretical effect of changes in inflammatory status on plasma protein binding and the expression of drug transporters/enzymes. Furthermore, ontogeny of SULT2A1 and P-gp is not incorporated in Simcyp. However, since SULT2A1 is mature after the neonatal period and we evaluated >3 months of age and the effect of P-gp in the model is modest, we do not expect this to have a major effect. Third, we assumed only inhibition and no induction by rifampicin when simulating the first 2 days of combined treatment, since available data suggest that rifampicin's (acute) inhibitory effect can be isolated from its (chronic) inductive effect by single dose administration in temporal proximity with the victim drug.[50] Interestingly, our simulations revealed only a minor impact of rifampicin-mediated inhibition on modeled moxifloxacin exposure in this scenario. As a result of the nonmechanistically incorporated

interaction, moxifloxacin pharmacokinetic predictions for coadministration with rifampicin in the period preceding full rifampicin-mediated induction are not possible with our PBPK model. Fourth, we know that the PK of drugs may differ between ethnicities and critically ill (TB meningitis) vs other patients, but our PBPK model predicted the PK of various and mixed populations appropriately. For Figure 4A and 4B (Indonesian patients at the end of their TB treatment), there was a small but systemic underprediction of moxifloxacin concentrations, compared to Figure 4C and 5 (patients in a Dutch TB referral hospital and patients with TB meningitis at the start of treatment). Therefore, we cannot exclude that our model slightly underpredicts moxifloxacin exposure in healthier patients with TB or healthy Indonesians in general. Fifth, there is no enterohepatic circulation incorporated in our model. We cannot exclude that the parent compound, formed in the gut lumen by deconjugation of moxifloxacin-glucuronide, might be reabsorbed. However, based on our conceptional overview of moxifloxacin excretion in Figure 8, 29% would end up in the feces as moxifloxacin. This is in line with the 25.4% found in feces by Stass et al,[23] limiting the probability of a large contribution of enterohepatic circulation. Finally, the magnitude in which described exposure differences impact moxifloxacin efficacy and pharmacodynamics was considered as outside the scope of this work.

Conclusion

In summary, we provided new insight into moxifloxacin pharmacokinetics, particularly regarding the limited role of P-gp in moxifloxacin transport and the relevant role of MRP2 in transport of moxifloxacin-glucuronide followed by hydrolysis in the gut. Furthermore, our simulations showed that moxifloxacin plasma concentrations restore after increasing the moxifloxacin dose to 600 mg during coadministration with rifampicin, and point to limited effects on moxifloxacin PK via rifampicin-mediated inhibition of P-gp and UGT1A1 as compared to rifampicin-mediated induction. Finally, various knowledge gaps were identified, which may be considered as avenues for further PBPK refinement.

Acknowledgments

We thank Simcyp (Certara) for free availability of the Simcyp simulator to academic institutions.

Conflicts of Interest

The authors declare no conflicts of interest.

Funding Information

This project was supported by a Radboudumc RIHS Junior Researcher Round Grant 2017.

Data Accessibility

Data available via Carlijn.Litjens@radboudumc.nl

References

1. WHO. Global tuberculosis report 2019. https://www.who.int/tb/publications/global_report/en/. Accessed December 11, 2019.
2. Tulkens PM, Arvis P, Kruesmann F. Moxifloxacin safety: an analysis of 14 years of clinical data. *Drugs R D*. 2012;12(2):71-100.
3. Soman A, Honeybourne D, Andrews J, Jevons G, Wise R. Concentrations of moxifloxacin in serum and pulmonary compartments following a single 400 mg oral dose in patients undergoing fibre-optic bronchoscopy. *J Antimicrob Chemother*. 1999;44(6):835-838.
4. *WHO consolidated guidelines on drug-resistant tuberculosis treatment*. Geneva: World Health Organization; 2019. Licence: CC BY-NC-SA 3.0 IGO.
5. Ruslami R, Ganiem AR, Dian S, et al. Intensified regimen containing rifampicin and moxifloxacin for tuberculous meningitis: an open-label, randomised controlled phase 2 trial. *Lancet Infect Dis*. 2013;13(1):27-35.
6. Donald PR. Cerebrospinal fluid concentrations of antituberculosis agents in adults and children. *Tuberculosis (Edinb)*. 2010;90(5):279-292.
7. Pranger AD, van der Werf TS, Kosterink JGW, Alffenaar JWC. The role of fluoroquinolones in the treatment of tuberculosis in 2019. *Drugs*. 2019;79(2):161-171.
8. Tachibana M, Tanaka M, Masubuchi Y, Horie T. Acyl glucuronidation of fluoroquinolone antibiotics by the UDP-glucuronosyltransferase 1A subfamily in human liver microsomes. *Drug Metab Dispos*. 2005;33(6):803-811.
9. Senggunprai L, Yoshinari K, Yamazoe Y. Selective role of sulfotransferase 2A1 (SULT2A1) in the N-sulfoconjugation of quinolone drugs in humans. *Drug Metab Dispos*. 2009;37(8):1711-1717.
10. Barot M, Gokulgandhi MR, Pal D, Mitra AK. In vitro moxifloxacin drug interaction with chemotherapeutics: implications for retinoblastoma management. *Exp Eye Res*. 2014;118:61-71.
11. Brillault J, De Castro WV, Harnois T, Kitzis A, Olivier JC, Couet W. P-glycoprotein-mediated transport of moxifloxacin in a Calu-3 lung epithelial cell model. *Antimicrob Agents Chemother*. 2009;53(4):1457-1462.
12. Doostdar H, Grant MH, Melvin WT, Wolf CR, Burke MD. The effects of inducing agents on cytochrome P450 and UDP-glucuronyltransferase activities in human HEPG2 hepatoma cells. *Biochem Pharmacol*. 1993;46(4):629-635.
13. Kern A, Bader A, Pichlmayr R, Sewing KF. Drug metabolism in hepatocyte sandwich cultures of rats and humans. *Biochem Pharmacol*. 1997;54(7):761-772.
14. Wenning LA, Hanley WD, Brainard DM, et al. Effect of rifampin, a potent inducer of drug-metabolizing enzymes, on the pharmacokinetics of raltegravir. *Antimicrob Agents Chemother*. 2009;53(7):2852-2856.
15. Dilger K, Greiner B, Fromm MF, Hofmann U, Kroemer HK, Eichelbaum M. Consequences of rifampicin treatment on propafenone disposition in extensive and poor metabolizers of CYP2D6. *Pharmacogenetics*. 1999;9(5):551-559.
16. Dilger K, Hofmann U, Klotz U. Enzyme induction in the elderly: effect of rifampin on the pharmacokinetics and pharmacodynamics of propafenone. *Clin Pharmacol Ther*. 2000;67(5):512-520.
17. Greiner B, Eichelbaum M, Fritz P, et al. The role of intestinal P-glycoprotein in the interaction of digoxin and rifampin. *J Clin Invest*. 1999;104(2):147-153.

18. Magis-Escurra C, Later-Nijland HM, Alffenaar JW, et al. Population pharmacokinetics and limited sampling strategy for first-line tuberculosis drugs and moxifloxacin. *Int J Antimicrob Agents*. 2014;44(3):229-234.
19. Nijland HM, Ruslami R, Suroto AJ, et al. Rifampicin reduces plasma concentrations of moxifloxacin in patients with tuberculosis. *Clin Infect Dis*. 2007;45(8):1001-1007.
20. Weiner M, Burman W, Luo CC, et al. Effects of rifampin and multidrug resistance gene polymorphism on concentrations of moxifloxacin. *Antimicrob Agents Chemother*. 2007;51(8):2861-2866.
21. Gumbo T, Louie A, Deziel MR, Parsons LM, Salfinger M, Drusano GL. Selection of a moxifloxacin dose that suppresses drug resistance in *Mycobacterium tuberculosis*, by use of an in vitro pharmacodynamic infection model and mathematical modeling. *J Infect Dis*. 2004;190(9):1642-1651.
22. Jamei M. Recent advances in development and application of physiologically-based pharmacokinetic (PBPK) models: a transition from academic curiosity to regulatory acceptance. *Curr Pharmacol Rep*. 2016;2:161-169.
23. Stass H, Kubitza D. Pharmacokinetics and elimination of moxifloxacin after oral and intravenous administration in man. *J Antimicrob Chemother*. 1999;43(suppl B):83-90.
24. Acocella G. Pharmacokinetics and metabolism of rifampin in humans. *Rev Infect Dis*. 1983;5(suppl 3):S428-S432.
25. Svensson RJ, Aarnoutse RE, Diacon AH, et al. A population pharmacokinetic model incorporating saturable pharmacokinetics and autoinduction for high rifampicin doses. *Clin Pharmacol Ther*. 2018;103(4):674-683.
26. Simcyp. 18.2 ed. https://www.certara.com/.
27. Bhatt DK, Mehrotra A, Gaedigk A, et al. Age- and genotype-dependent variability in the protein abundance and activity of six major uridine diphosphate-glucuronosyltransferases in human liver. *Clin Pharmacol Ther*. 2019;105(1):131-141.
28. Ladumor MK, Bhatt DK, Gaedigk A, et al. Ontogeny of hepatic sulfotransferases and prediction of age-dependent fractional contribution of sulfation in acetaminophen metabolism. *Drug Metab Dispos*. 2019;47(8):818-831.
29. Sager JE, Yu J, Ragueneau-Majlessi I, Isoherranen N. Physiologically based pharmacokinetic (PBPK) modeling and simulation approaches: a systematic review of published models, applications, and model verification. *Drug Metab Dispos*. 2015;43(11):1823-1837.
30. Stass H, Dalhoff A, Kubitza D, Schuhly U. Pharmacokinetics, safety, and tolerability of ascending single doses of moxifloxacin, a new 8-methoxy quinolone, administered to healthy subjects. *Antimicrob Agents Chemother*. 1998;42(8):2060-2065.
31. Sullivan JT, Woodruff M, Lettieri J, et al. Pharmacokinetics of a once-daily oral dose of moxifloxacin (Bay 12–8039), a new enantiomerically pure 8-methoxy quinolone. *Antimicrob Agents Chemother*. 1999;43(11):2793-2797.
32. Lettieri J, Vargas R, Agarwal V, Liu P. Effect of food on the pharmacokinetics of a single oral dose of moxifloxacin 400mg in healthy male volunteers. *Clin Pharmacokinet*. 2001;40 Suppl 1:19-25.
33. Stass H, Lettieri J, Vanevski KM, et al. Pharmacokinetics, safety, and tolerability of single-dose intravenous moxifloxacin in pediatric patients: dose optimization in a phase 1 study. *J Clin Pharmacol*. 2019;59(5):654-667.
34. Thee S, Garcia-Prats AJ, Draper HR, et al. Pharmacokinetics and safety of moxifloxacin in children with multidrug-resistant tuberculosis. *Clin Infect Dis*. 2015;60(4):549-556.
35. Te Brake LH, van den Heuvel JJ, Buaben AO, et al. Moxifloxacin is a potent in vitro inhibitor of OCT- and MATE-mediated transport of metformin and ethambutol. *Antimicrob Agents Chemother*. 2016;60(12):7105-7114.
36. Ballow C, Lettieri J, Agarwal V, Liu P, Stass H, Sullivan JT. Absolute bioavailability of moxifloxacin. *Clin Ther*. 1999;21(3):513-522.
37. Rodgers T, Rowland M. Physiologically based pharmacokinetic modelling 2: predicting the tissue distribution of acids, very weak bases, neutrals and zwitterions. *J Pharm Sci*. 2006;95(6):1238-1257.
38. Gufford BT, Robarge JD, Eadon MT, et al. Rifampin modulation of xeno- and endobiotic conjugating enzyme mRNA expression and associated microRNAs in human hepatocytes. *Pharmacol Res Perspect*. 2018;6(2):e00386.
39. Te Brake LH, Russel FG, van den Heuvel JJ, et al. Inhibitory potential of tuberculosis drugs on ATP-binding cassette drug transporters. *Tuberculosis (Edinb)*. 2016;96: 150-157.
40. Cheng Y, Prusoff WH. Relationship between the inhibition constant (K1) and the concentration of inhibitor which causes 50 per cent inhibition (I50) of an enzymatic reaction. *Biochem Pharmacol*. 1973;22(23):3099-3108.
41. Cao L, Greenblatt DJ, Kwara A. Inhibitory effects of selected antituberculosis drugs on common human hepatic cytochrome P450 and UDP-glucuronosyltransferase enzymes. *Drug Metab Dispos*. 2017;45(9):1035-1043.
42. Neuhoff S, Yeo KR, Barter Z, Jamei M, Turner DB, Rostami-Hodjegan A. Application of permeability-limited physiologically-based pharmacokinetic models: part II - prediction of P-glycoprotein mediated drug-drug interactions with digoxin. *J Pharm Sci*. 2013;102(9):3161-3173.
43. Imai Y, Asada S, Tsukahara S, Ishikawa E, Tsuruo T, Sugimoto Y. Breast cancer resistance protein exports sulfated estrogens but not free estrogens. *Mol Pharmacol*. 2003;64(3):610-618.
44. Suzuki M, Suzuki H, Sugimoto Y, Sugiyama Y. ABCG2 transports sulfated conjugates of steroids and xenobiotics. *J Biol Chem*. 2003;278(25):22644-22649.
45. Kaneko M, Aoyama T, Ishida Y, et al. Lack of ethnic differences of moxifloxacin and metabolite pharmacokinetics in East Asian men. *J Pharmacokinet Pharmacodyn*. 2018;45(2):199-214.
46. Roberts MS, Magnusson BM, Burczynski FJ, Weiss M. Enterohepatic circulation: physiological, pharmacokinetic and clinical implications. *Clin Pharmacokinet*. 2002;41(10): 751–790.
47. Ahmed S, Vo NT, Thalhammer T, Thalhammer F, Gattringer KB, Jager W. Involvement of Mrp2 (Abcc2) in biliary excretion of moxifloxacin and its metabolites in the isolated perfused rat liver. *J Pharm Pharmacol*. 2008;60(1):55-62.
48. Hamoud AR, Weaver L, Stec DE, Hinds TD, Jr. Bilirubin in the liver-gut signaling axis. *Trends Endocrinol Metab*. 2018;29(3):140-150.
49. Niemi M, Backman JT, Fromm MF, Neuvonen PJ, Kivisto KT. Pharmacokinetic interactions with rifampicin: clinical relevance. *Clin Pharmacokinet*. 2003;42(9):819-850.
50. Reitman ML, Chu X, Cai X, et al. Rifampin's acute inhibitory and chronic inductive drug interactions: experimental and model-based approaches to drug-drug interaction trial design. *Clin Pharmacol Ther*. 2011;89(2):234-242.

Supplemental Information

Additional supplemental information can be found by clicking the Supplements link in the PDF toolbar or the Supplemental Information section at the end of web-based version of this article.